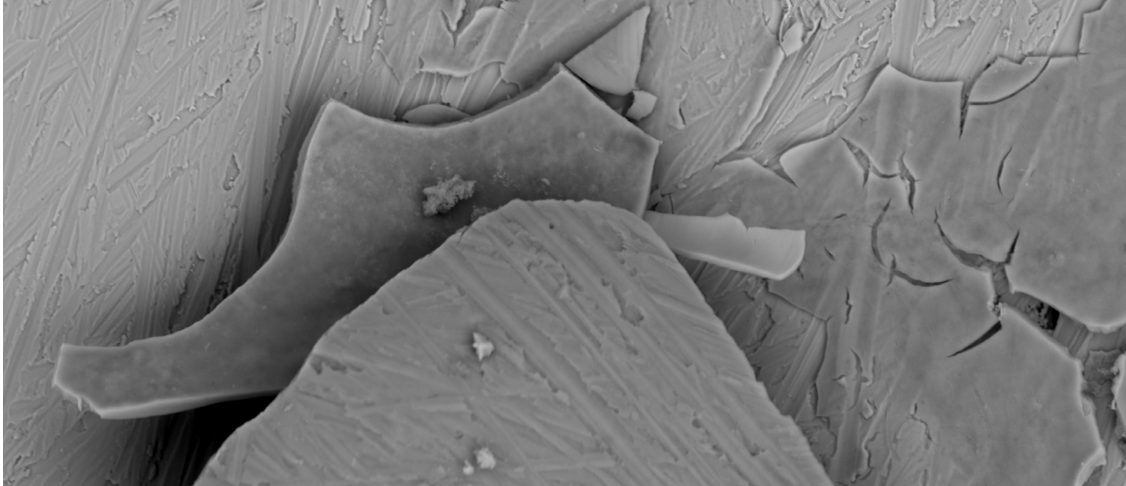




CHALMERS
UNIVERSITY OF TECHNOLOGY



Low Temperature Synthesis of Iron Oxide Films via Precipitation from Aqueous Solution for Suppression of Radioactivity Buildup in Nuclear Power Plants

Degree project report in Chemical Engineering

Petter Jacobsson

DEPARTMENT OF CHEMISTRY AND CHEMICAL ENGINEERING

CHALMERS UNIVERSITY OF TECHNOLOGY
Gothenburg, Sweden 2024
www.chalmers.se

DEGREE PROJECT REPORT 2024

Low Temperature Synthesis of Iron Oxide Films via Precipitation from Aqueous Solution for Suppression of Radioactivity Buildup in Nuclear Power Plants

Petter Jacobsson



CHALMERS
UNIVERSITY OF TECHNOLOGY

DEPARTMENT OF CHEMISTRY AND CHEMICAL ENGINEERING
CHALMERS UNIVERSITY OF TECHNOLOGY
Gothenburg, Sweden 2024

Low Temperature Synthesis of Iron Oxide Films via Precipitation from Aqueous Solution for Suppression of Radioactivity Buildup in Nuclear Power Plants

Petter Jacobsson

© Petter Jacobsson, 2024.

Supervisor: Christine Geers, Department of chemistry and chemical engineering

Jiaxin Chen, Studsvik

Examiner: Jan Froitzheim, Department of chemistry and chemical engineering

Degree project report 2024

Department of chemistry and chemical engineering

Chalmers University of Technology

SE-412 96 Gothenburg

Sweden

Telephone +46 31 772 1000

Cover: Backscatter image of deposited hematite.

Gothenburg, Sweden 2024

Low Temperature Synthesis of Iron Oxide Films via Precipitation from Aqueous Solution for Suppression of Radioactivity Buildup in Nuclear Power Plants

Petter Jacobsson
Department of chemistry and chemical engineering
Chalmers University of Technology

Abstract

Uptake of radioactive $^{60}\text{Co}^{2+}$ in nuclear reactor cooling loops poses a problem in nuclear power plants. Unattended oxide films on 316L stainless steel results in an outer formation of iron-nickel spinel crystalites and inner iron-chromium spinel layer. The outer crystalites incorporate the radioactive isotope ^{60}Co , which has a half life of 5.3 years, from cooling water. The issue is as of today addressed through zinc injection or the patented Hi-F Coat, the latter is a electroless deposition method of hematite and magnetite. The Hi-FC is a subject of modification to exclude chemicals harmful to the user and the environment. Hematite does not allow for uptake of $^{60}\text{Co}^{2+}$ and therefore this study will aim to via electroless deposition, deposit a hematite layer for applications in nuclear power plants cooling loops. A successful implementation of this will lower the radiation dose experienced within the cooling loop with up to 90% and drastically reduce the associated health risks and maintenance costs.

Keywords: Electroless deposition, Co uptake, Hematite

Contents

1	Introduction	1
1.1	Background	1
1.2	Cobalt deposition behavior	1
1.3	Electroless deposition	2
1.4	Electroplating	2
1.5	Reabsorption suppression methods	3
1.5.1	Zinc injection	3
1.5.2	Hi-F Coat	3
1.6	Selection of chemicals	4
1.6.1	Suitability for the use in nuclear power plants	4
1.6.2	Hydrazine	4
1.7	Aim	5
2	Theory	7
2.1	Iron ion source	7
2.1.1	Iron(II)oxalate	7
2.1.2	Iron(II)acetate	8
2.1.3	Iron(II)formate	8
2.1.4	Elemental iron	9
2.2	Oxidation agent	9
2.3	pH controller	9
2.3.1	Hydrazine	9
2.3.2	KOH	10
2.3.3	Ammonia solution	10
2.4	Reactions	10
2.5	Metals present	11
2.5.1	18-8 Stainless steel wire	11
2.5.2	Zinc wire	11
3	Experimental	13
3.1	Setup	13
3.2	316L Stainless steel	13
3.3	Samples	14
3.4	Wire	14
3.4.1	18-8 Stainless steel	14
3.4.2	Zinc wire	15

3.5	In situ Iron(II)formate preparation	15
3.6	General method	15
3.7	Scanning Electron Microscope analysis	16
3.8	X-ray diffraction	16
3.9	Table of chemicals	16
4	Results	17
4.1	Iron-oxalat	17
4.2	Iron(II)acetate	17
4.2.1	Zinc wire	17
4.2.1.1	KOH and ammonia solution	17
4.2.1.2	Hydrazine	19
4.3	In situ iron formate	20
4.3.1	18-8 Stainless steel wire	20
4.3.1.1	KOH	20
4.3.1.2	Ammonia solution	21
4.3.1.3	Hydrazine	23
5	Discussion	25
5.1	Sample position and setup	25
5.2	Hi-F Coat replication	25
5.3	Ferrous ion source	26
5.3.1	Fe(II)Oxalate paint	26
5.3.2	Iron(II)acetate	26
5.3.3	Iron(II)formate	26
5.4	Oxidation agent	26
5.5	pH controller	26
5.5.1	Ammonia solution	26
5.5.2	KOH	27
5.6	Zinc dissolution presence	27
6	Conclusion	29
6.1	Hi-FC reproduction	29
6.2	pH adjuster	29
6.3	Iron source	29
	Bibliography	31

1

Introduction

1.1 Background

In nuclear power plants, the cooling water carries small amounts of radioactive Cobalt ions. The $^{60}\text{Co}^{2+}$ is absorbed into the oxide scale of the stainless steel pipes in the plant and has a half life of 5.3 years. Over 90% of the radioactive dose experienced within the cooling loop under normal operating conditions comes from radioactive corrosion products such as ^{60}Co incorporated in the iron-nickel oxides at the surface.[1] To combat the rising amount of radiation outside the core, chemical decontamination is used in many Boiling Water Reactors (BWR).[2, 3] After the decontamination, if no additional treatment is applied, the rate of deposition of $^{60}\text{Co}^{2+}$ is very high and already after a few cycles the radioactivity of the pipes is back at its previous state.[3] The reabsorption of ^{60}Co after a chemical decontamination can be limited by a few different measures.

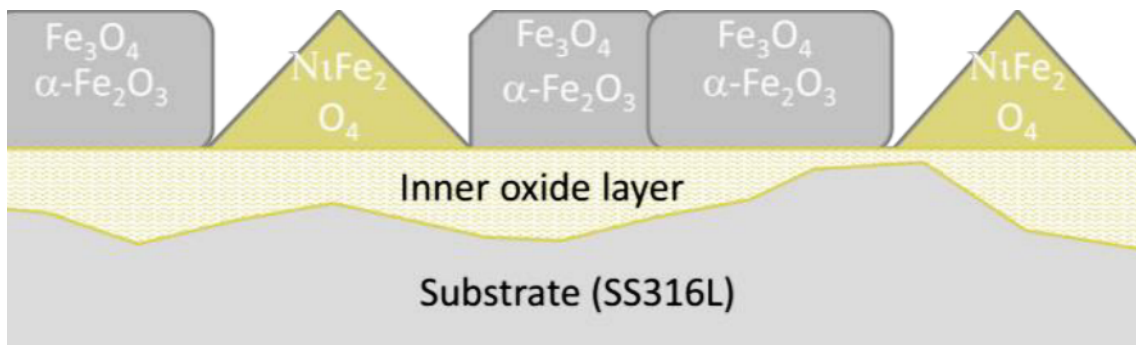


Figure 1.1: Generic oxide film of 316L stainless steel [3]

Outer oxide layer consists of Fe-Ni and Fe oxide grains, inner oxide layer mostly a mixed spinel M_3O_4 where M is either one or more of Fe, Ni and Cr.[3]

1.2 Cobalt deposition behavior

The cobalt deposits onto the stainless steel by binding at the octahedral lattice sites of the inverse spinel where nickel normally resides.[4] Iron-nickel oxides like magnetite forms a inverse spinel structure while hematite will form a trigonal-hexagonal scalenohedral structure where cobalt does not preferentially resides.

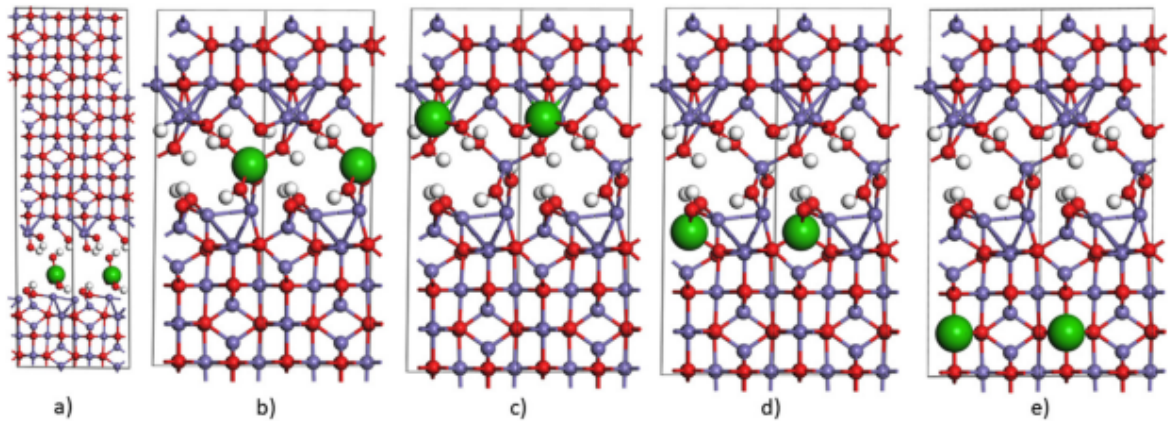


Figure 1.2: Inverse spinel structure of magnetite with hydroxolated grain boundaries. Iron in blue, oxygen in red and M in green.[4]

Illustrated in fig. 1.2 a metal ion, in this case M is cobalt, may bind to the surface and diffuses along surfaces and grain boundaries where it gets incorporated into the growing oxide upon aging.

1.3 Electroless deposition

The method of electroless deposition in this case involves oxidizing iron to Fe^{II} or Fe^{III} oxides and let the insoluble oxides precipitate onto the material. This process involves three main components:

- Ferrous ions
- Oxidizing agent
- pH adjuster

The process of electroless deposition relies on slowly oxidizing the iron ions to get an even coating and not letting the iron precipitate too fast in the solution. The process must be carefully designed to achieve this.[2]

1.4 Electroplating

A common way to deposit coatings onto metal or other conductive substrates is electroplating. It works by applying a potential over solution and substrate to attract the desired ions suspended in the solution onto the substrate where reaction occurs, mostly the ions are suspended in aqueous solution. With this method a very thick layer can be applied though it can be a costly option depending on the scale in which it is applied.[5] To then establish the required hematite coating, the iron deposited needs to be reoxidated.

1.5 Reabsorption suppression methods

1.5.1 Zinc injection

Injection of zinc into the cooling water is widely used in Pressurized Water Reactor (PWR) but also implemented in BWR. It works by incorporation of Zn^{2+} into all surfaces and grain boundaries of the outer oxide species and prevents radioactive Co^{2+} to stick to the surface.[6] In fig. 1.2, M may also be Zn^{2+} but would then reside in the hydroxylated interfaces, disallowing cobalt to reach its preferential site and there through out competing the Co^{2+} . Zinc injection is the most widely used method to prevent ^{60}Co from deposit on the stainless steel.[4] This method has been in use since the 1970's in the US and first implemented in Sweden 1999 [7].

1.5.2 Hi-F Coat

The Hitachi ferrite coating method (Hi-F) is a form of *electroless deposition* of iron oxide film using iron formate ($\text{Fe}(\text{HCOO})_2$) as the ferrous ions, hydrogen peroxide (H_2O_2) as the oxidation agent and adjusts the pH with hydrazine (N_2H_4). Most chemicals are already present if the HOP (Hydrazine, Oxalic acid and Potassium) decontamination process is used, where hydrogen peroxide is used as a catalyst. All residual components of the Hi-F Coat can be decomposed into water and gases.[2] The Hi-F Coat was further developed and OHi-F Coat was created, which was more effective (fig. 1.4). The main difference is that OHi-F Coat produces mainly hematite rather than just magnetite as in Hi-F Coat, as shown in fig. 1.5. Shown in fig. 1.3 is the test rig used for development of Hi-FC and OHi-FC.[8]

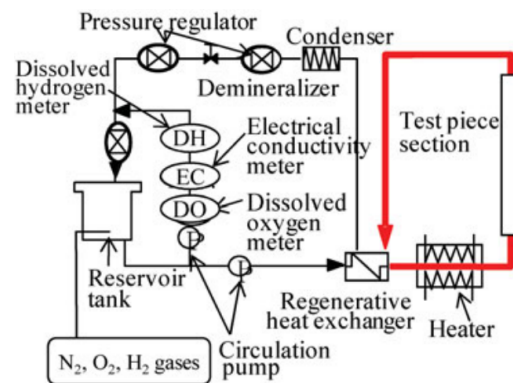


Figure 1.3: Test rig used in development of Hi-FC and OHi-FC [8]

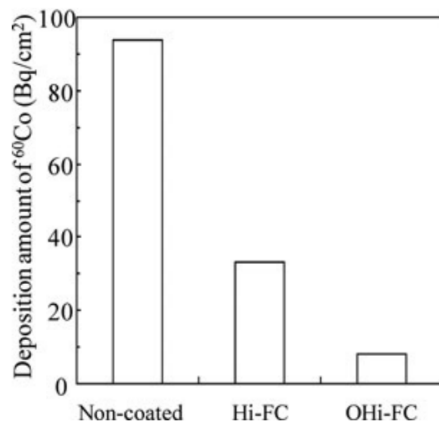


Figure 1.4: Cobalt deposition test conducted on the oxide films produced through Hi-FC and OHi-FC, showing the effectiveness of a iron oxide scale, particular OHi-FC [8]

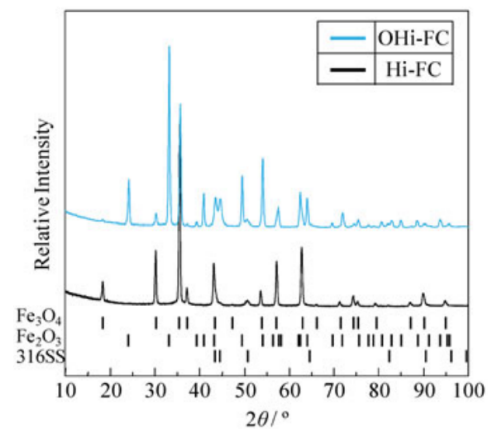


Figure 1.5: XRD analysis of Hi-FC and OHi-FC showing Hi-FC is a magnetite coating and OHi-FC is mainly hematite with some magnetite (Fe_3O_4 is magnetite and Fe_2O_3 is hematite) [8]

1.6 Selection of chemicals

1.6.1 Suitability for the use in nuclear power plants

For the use in nuclear power plant cooling loops there are a few requirements regarding such matters as the longevity of the stainless steel pipes, minimizing the nuclear waste as well as considering the cost [3]:

1. Ensuring absence of highly corrosive chemicals
2. Limiting the amount of time the reactor is on low power
3. Ability to decompose any chemicals used in the process into disposable components
4. Process must not damage the system in any way

1.6.2 Hydrazine

Hydrazine used in the Hi-F method brings along a few health and safety concerns. The Safety Data Sheet lists following in the most dangerous category; serious eye damage, skin sensitisation, acute and chronic aquatic toxicity. If ingested or inhaled it may cause death by mainly targeting organs such as the nerve system, blood, liver, kidneys and lungs. Along with these acute harmful to a human its classified in the second most dangerous carcinogenicity category. In high concentrations hydrazine is also flammable in both liquid and vapor state.[9] Another concern is the environmental impact if accidental release into groundwater. Hydrazine reacts

rapidly in air mostly with ozone if released into the atmosphere. Highly diluted in water however the degradation is slow and at low concentrations, though still toxic, lifespan may be significantly longer depending on water composition.[10]

1.7 Aim

The aim of this study is to investigate methods of suppressing cobalt uptake within the cooling loop of nuclear power plants. Mainly through depositing hematite onto stainless steel by replicating and modifying the Hi-F Coat. No testing of uptake behavior will be conducted.

2

Theory

This study will further discuss catalytsless electroless deposition of hematite on 316L stainless steel.

The theory of electroless deposition involves three main components; ferrous ions, an oxidation agent and pH controller. This to first put the iron into Fe^{II} and then to slowly oxidize it into Fe^{III} and deposit onto the stainless steel as magnetite or iron hydroxides, the pH is controlled to the point where oxidation is not rapid (rapid precipitation marked in blue in fig. 2.1). Then the magnetite and iron hydroxides is baked into hematite.[2] The patented Hi-F method uses iron dissolved in formic acid, hydrogen peroxide and hydrazine, this could be modified by using other chemicals and adjusting the rest to fit the criteria.

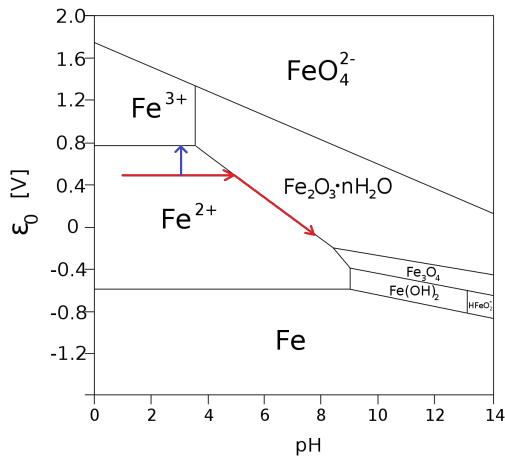


Figure 2.1: Pourbaix diagram for iron at standard conditions. With the intended reaction path marked in red. [11]

Pourbaix diagram for iron shows which oxidation states of iron are stable depending on pH and chemical potential, the diagram uses hydrogen standard electrode potential as reference 0. As shown in fig. 2.1, controlling the pH makes it possible to hit and stay at the point where both Fe^{2+} and Fe_2O_3 are at equilibrium. The red arrow shows the ideal path by adding a perfect amount of pH controlling agent, blue arrow represents rapid precipitation. Although the diagram is for 1M iron solution at standard conditions, it is still applicable at 90°C at a much lower concentration as the behavior in general will not change only shift along the axis.

2.1 Iron ion source

2.1.1 Iron(II)oxalate

A possibly viable source of iron ions could be iron oxalate $\text{FeC}_2\text{O}_4(\text{H}_2\text{O})_x$ (fig. 2.2). The iron is already in Fe^{II} and the organic part is baked off when heat treated at

280°C. It is an easy to come by and relatively safe source of iron. If it could be dissolved in acid it might be an alternative. Otherwise it is applied as paint pigment and then available as slurry coating.

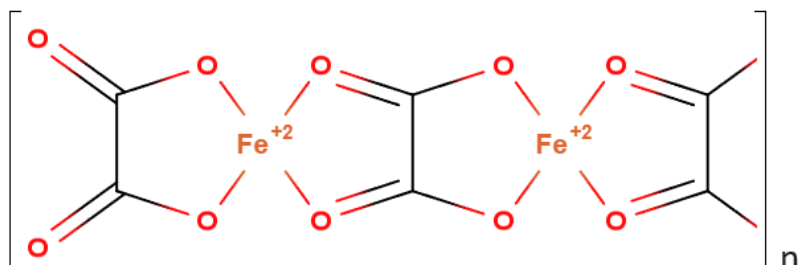


Figure 2.2: Molecular polymer forming structure of Iron(II)oxalate with complexing bonds.

2.1.2 Iron(II)acetate

Iron(II)acetate $\text{Fe}^{\text{II}}(\text{CH}_3\text{COO})_2$ (fig. 2.3) is an other metal organic alternative source of iron ions that is already in Fe^{II} . The powder is safe to handle although problems arise when storing, Iron(II)acetate is reactive with air and if not stored properly may react into Iron(III)acetate and oxides. This may pose difficulties to achieve repeatable results.

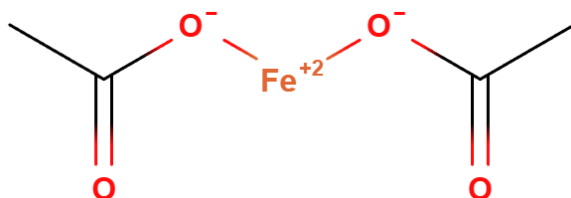


Figure 2.3: The molecular structure of $\text{Fe}^{\text{II}}(\text{CH}_3\text{COO})_2$

2.1.3 Iron(II)formate

Iron(II)formate $\text{Fe}^{\text{II}}(\text{HCOO})_2$ (fig. 2.4) can be produced *in situ* according to eq. (2.1) by dissolving pure iron in formic acid. The process may be slow and to ensure the Fe^{2+} does not react into Fe^{3+} an airlock should be used to let the gas produced escape without letting too much oxygen in.



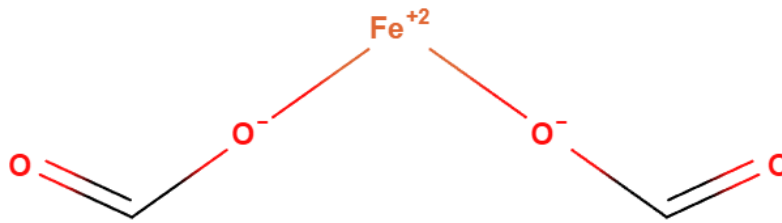


Figure 2.4: The molecular structure of $\text{Fe}^{\text{II}}(\text{HCOO})_2$

2.1.4 Elemental iron

Pure iron could be dissolved in acid to create Fe^{2+} in solution. This way has the advantage that it is in principle a reliable way of obtaining the iron ions. Dissolving elemental iron in formic acid (see eq. (2.1)) was the source of iron ions used in the Hi-F method [2]. The acid used may be organic for it to decompose when baking the sample after exposure, highly corrosive ions from mineral acids should not be introduced. Highly pure iron in its elemental form is difficult to produce and therefore might be a costly alternative.

2.2 Oxidation agent

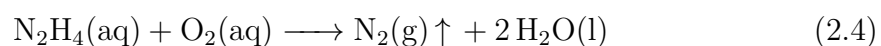
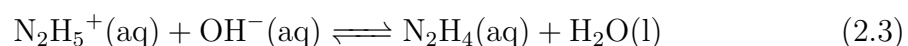
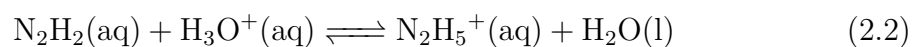
Where as the other components have many alternatives, hydrogen peroxide has mostly advantages. Relatively safe to handle and decomposes disposable components. The amount must be adjusted to compliment the other components and in some cases it might be possible to completely exclude if an oxidative environment is already achieved.

2.3 pH controller

In all cases brought up the iron source dissolution will start the experiment under acidic conditions and will therefore need an alkaline pH controlling agent.

2.3.1 Hydrazine

The use of hydrazine to control the pH has another advantage other then just bringing the pH back up to the required pH but also, hydrazine is a strong reducing agent. The reducing properties of hydrazine aid the fine tuning of the process and allows the deposition to take place even at neutral pH [2].



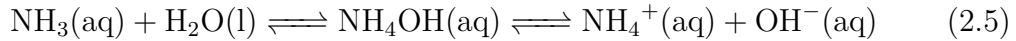
Shown in eqs. (2.2) and (2.3) is the pH controlling reactions of hydrazine in aqueous solution, with a pKa of 7.96 at standard conditions will it make the solution alkaline.[12] Seen in eq. (2.4) is the strong reductive properties of hydrazine.

2.3.2 KOH

Any hydroxide is the most direct method of increasing pH in the solution. In the case of application in BWR cooling loops, no ions prone to inducing stress corrosion cracking may be introduced. Therefore is potassium a viable option cause of its larger ionic size and inability to penetrate the steel microstructure.

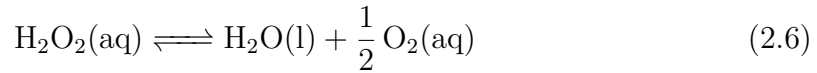
2.3.3 Ammonia solution

Ammonia solution is NH_3 dissolved in water. The ammonia in water is in equilibrium with the ammonium ion NH_4^+ as seen in eq. (2.5) and will produce an alkaline solution, at standard conditions pKa is 9.25. The equilibrium in eq. (2.5) is highly temperature and pH dependent.[13]

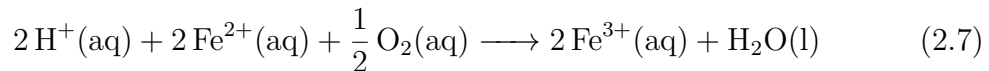


2.4 Reactions

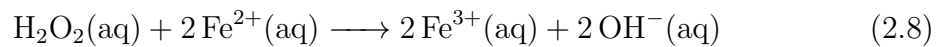
Hydrogen peroxide oxidative reaction in water



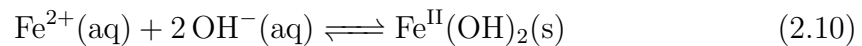
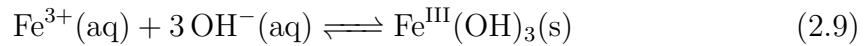
oxidizes Fe^{2+} into Fe^{3+} in an acid environment according to



or the iron ions react directly with hydrogen peroxide to form Fe^{3+} ions.



Iron ions reacts with free hydroxide groups and forms an iron hydroxide.



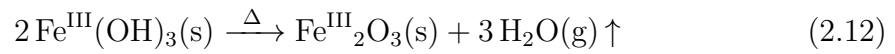
Several of the reactions are very pH dependent and these equilibriums is ultimately what decides the optimal ratios of each component when running an exposure.

$\text{Fe}(\text{OH})_3$ is insoluble in water and will appear as fine precipitation suspended in solution that is able to adhere to the activated surface of the sample.

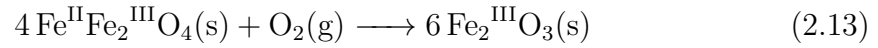
Magnetite is coprecipitated onto the surface of the metal according to:



Hydroxylated iron that was deposited onto the surface of the stainless steel is baked into hematite after the exposure.



Magnetite is during the heat treatment transformed into hematite: [14].



2.5 Metals present

With this setup the steel wire is the only solid component in direct contact with the sample and partly submersed in the solution, the wire must be chosen with care as it may interfere with the result.

2.5.1 18-8 Stainless steel wire

Stainless steel wire of type 18-8 has very similar properties to the 316 stainless steel sample and should not interfere with the chemistry in the solution. The wire must be analyzed to determine the composition and be properly cleaned before use.

2.5.2 Zinc wire

Using a zinc wire to hang the sample introduces a new metal into the solution, a less noble metal that in acid solution will dissolve and Zn^{2+} ions will be in solution under H_2 evolution together with Fe^{2+} ions. Though introducing new metal ions may seem like contamination, it can work as a sacrificial anode and oxidation buffer to achieve the slightly oxidative environment that is sought after. Zinc injection is at the moment the most used method of ^{60}Co uptake suppression and therefore already present in many cooling loops. [6]

3

Experimental

3.1 Setup

The exposure setup, seen in fig. 3.1, was a temperature controlled silicone oil bath on a *IKA C-MAG HS7 digital* hotplate with a flask containing the continuously stirred solution suspended in the oil. Temperature and pH in the solution was continuously monitored with the *VWR pH110M* pH meter. The sample was hung using a metal wire, careful neither to let it be in direct contact with the pH meter nor the bottom, marked as position 1 or put lying down at the bottom of the flask marked as position 2. Silicone oil was used for its very good heat transfer properties and ability to maintain a stable temperature within the solution.

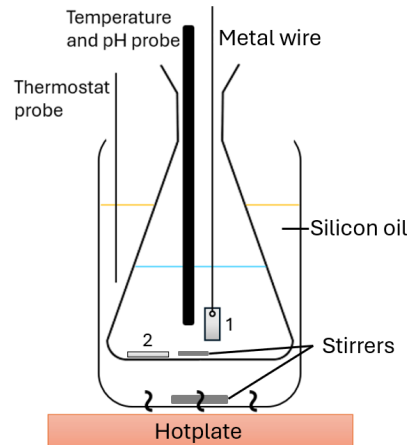


Figure 3.1: Exposure setup, markings 1 and 2 corresponds to sample positions during exposure.

3.2 316L Stainless steel

Stainless steel type 316L is a high performance austenitic low carbon stainless steel. Specifications listed in table 3.1

Element	Weight percent
C	0.03
N	0.10
Cr	16-18
Ni	10-14
Mo	2-3

Table 3.1: Specifications for 316L stainless steel, Iron content not specified [15]

3.3 Samples

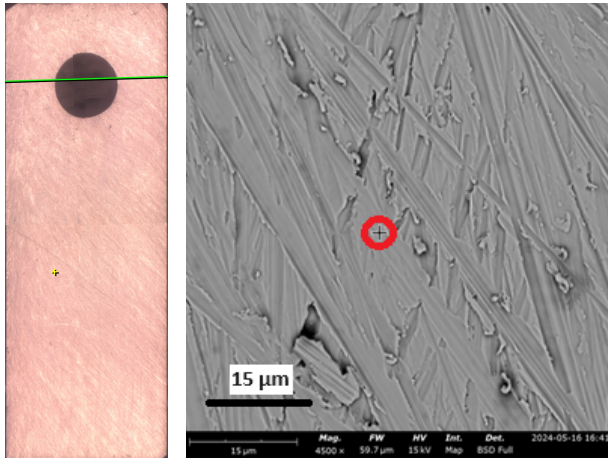


Figure 3.2: Surface of sample after grinding emulating the surface roughness of a cooling pipe. Optical (left) and backscatter image (right)

Element	Atomic Conc.	Weight Conc.
Fe	64.6	64.4
Cr	18.8	17.5
Ni	12.1	12.7
Mo	1.9	3.3
Mn	1.7	1.7
Si	0.9	0.5

Table 3.2: EDS measurement of the prepared sample

Samples made of 316L stainless steel delivered by Studsvik and cut up to appropriate size. To emulate the surface roughness of a cooling pipe in use, 500 grit SiC paper was used to create a fresh and flat surface. Surface roughness of sample after grinding shown in fig. 3.2 and composition seen in table 3.2 was compared to table 3.1 with little to no trace of contamination.

3.4 Wire

3.4.1 18-8 Stainless steel

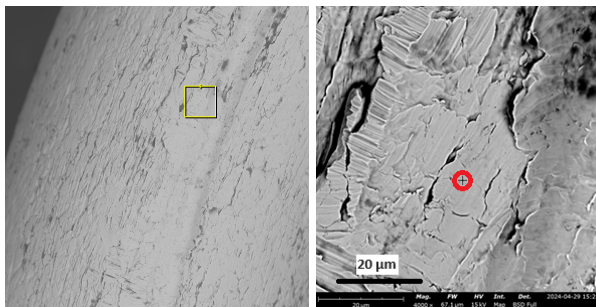


Figure 3.3: Backscatter images of the 18-8 stainless steel wire.

Element	Atomic Conc.	Weight Conc.
Fe	71.1	72.0
Cr	18.9	17.8
Ni	7.8	8.3
Mn	0.8	0.8
Co	0.7	0.8
Si	0.7	0.4

Table 3.3: Atomic and weight concentrations of the elements found in the stainless steel wire measured via EDS.

The 18-8 stainless steel wire (fig. 3.3) was analyzed to ensure its composition and impurities. It had the expected composition, seen in table 3.3, and trace elements that was also found in the sample.

3.4.2 Zinc wire

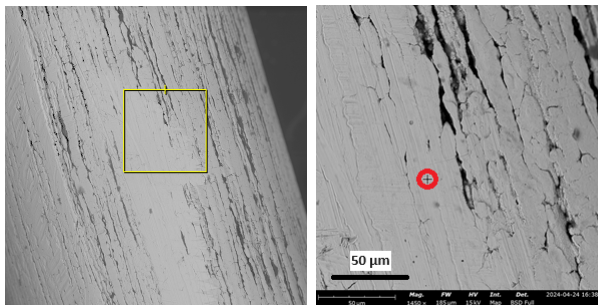


Figure 3.4: Backscatter images of the Zinc wire.

Element	Atomic Conc.	Weight Conc.
Zn	85.7	88.0
Fe	13.1	11.4
P	1.3	0.6

Table 3.4: EDS measurement of the zinc wire.

The wire referred to as zinc wire (fig. 3.4) is composed of mainly zinc and iron (see table 3.4). Its original use is soldering.

3.5 In situ Iron(II)formate preparation

Pure iron powder was added to formic acid in an e-flask. To prevent the iron to oxidize to Fe(III) and still letting hydrogen gas produced escape, an airlock was connected to the flask. To fully let it react, the solution should be left at least 24h or until no more iron powder can be spotted. The solution should be stored under an airlock to not create over pressure if it further reacts nor letting it react with the oxygen in the air.

3.6 General method

Stainless steel 316L $14.5 \times 5 \times 1.5$ mm with a 1.9 mm diameter hole samples were prepared by grinding each side with a 500 grit SiC paper, making sure to create a flat and fresh surface. Just before exposure the sample was cleaned with acetone and ethanol. The iron source was added to 150 ml of DI water and heated up to 90°C and then the sample was put in, pH at this was dependent on which iron source was used. If an oxidizing agent was used it was added just before adjusting the pH to intended value. After 4 hours the sample was taken out of the solution and left to air dry in room temperature. Not removing the wire in contact with the sample, it was put into a box furnace for one hour at 280°C and the taken out to cool off

in room temperature. The coating was analyzed with the *Phenom ProX* Scanning Electron Microscope and XRD.

3.7 Scanning Electron Microscope analysis

The samples were primarily analyzed in *Phenom ProX* SEM to observe structure and composition. A focused electron beam is directed onto the surface of the sample in a vacuum. Electrons hitting the surface scatters back and can be measured. Oxides crate a darker contrast in backscatter mode compared to metallic areas.[16] The acceleration voltage determines which atom orbital electron energy levels can be excited to generate detector response, for the analysis an acceleration voltage of 15 keV is used.

3.8 X-ray diffraction

XRD is a technique to help characterizing the crystalline structures of the sample.[17] A monochromatic X-ray beam at an angle θ is intericting with the sample and creates a scattering pattern at the detector.[18] Measurements are taken between $2\theta = 10^\circ$ and $2\theta = 90^\circ$ at 0.02° increments. Copper source with operating wave length of 1.54060 is used.

3.9 Table of chemicals

Chemical	Formula	Make	Comments
Ammonia solution	NH ₃	EMSURE	25%
Hydrazine	N ₂ H ₂	thermo scientific	Hydrazine hydrate 55% (Hydrazine 35%)
Potassium hydroxide	KOH	EMSURE	Pellet
Hydrogen peroxide	H ₂ O ₂	VWR	3% stabilized with phosphates
Formic acid	CH ₂ O ₂	VWR	98%
Iron(II)oxalate	FeC ₂ O ₄ · 2 H ₂ O	thermo scientific	99%
Iron(II)acetate	Fe(CH ₃ COO) ₂	Aldrich	95%
Iron powder	Fe	thermo scientific	-20 mesh 99% (metals basis)

4

Results

4.1 Iron-oxalat

Iron oxalat would be able to be a source of iron ions, the dissolution properties were tested to determinate its suitability.

0.0223 grams of oxalat was put into 30 milliliters of DI water, which would result in a desired concentration of iron ions, and put on a hot plate with a magnetic stirrer. Acetic acid was slowly added. When 22 grams of acetic acid had been added and the solution reached 80°C with an acidity around pH 2, the attempt was aborted as very little of the oxalat had dissolved and iron oxalate was deemed unfit for the application.

4.2 Iron(II)acetate

Iron(II)acetate was successfully dissolved in DI water and a drop of formic acid was added to the already acidic solution to further make sure it was properly dissolved. In total 9 mg of iron(II)acetate were added to 150 ml of DI water to create a concentration of 0.358 mmol/l of iron ions in the solution. *A 10th of what used in the Hi-F method [2] due to low surface area.*

4.2.1 Zinc wire

4.2.1.1 KOH and ammonia solution

Potassium hydroxide was tried as the pH controller component but its strong alkaline properties created a too oxidative environment and KOH was deemed unfit i combination with iron(II)acetate and hydrogen peroxide as the iron precipitated rapidly. As seen in fig. 4.1, analyzing proved that some of the iron ions had deposited but to an unsatisfactory amount. Ammonia solution produced similar results.

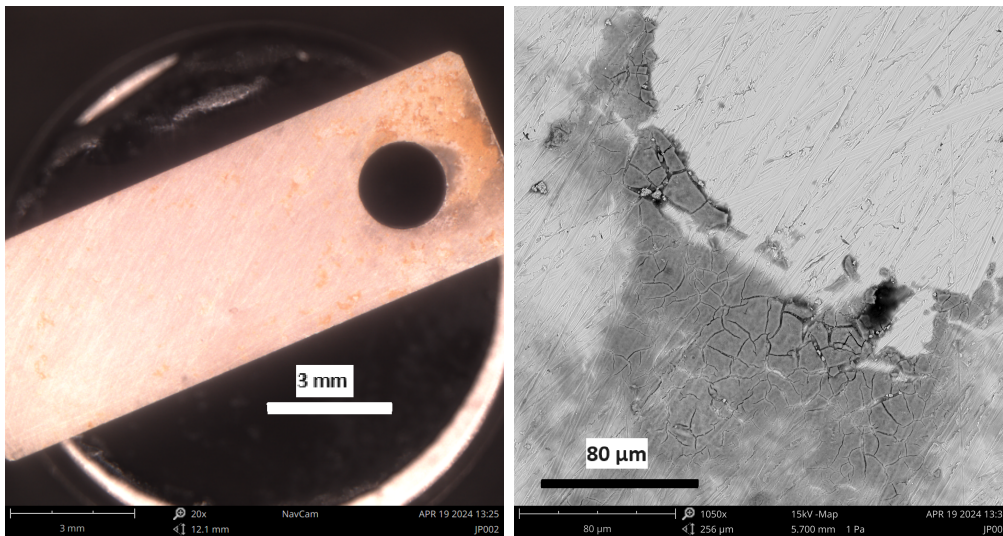


Figure 4.1: Deposition on stainless steel using KOH as the pH controller was present though scarce. Left: Optical microscope. Right: Backscatter image, the darker areas are oxide scales.

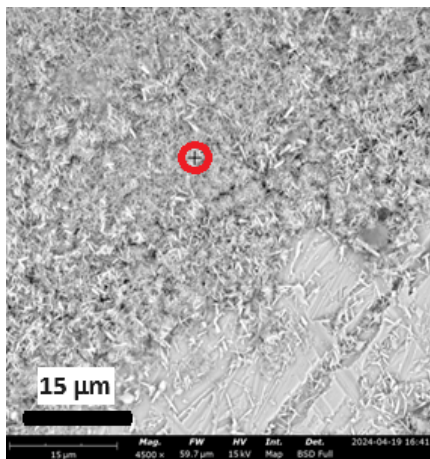


Figure 4.2: Backscatter image for spot analysis of sample using ammonia solution as pH adjuster at close proximity to where the wire was situated.

Element	Atomic Conc.	Weight Conc.
Zn	41.2	58.9
O	34.9	12.2
Fe	18.8	22.9
Cr	3.5	4.0
Ni	0.8	1.0

Table 4.1: EDS measurement showing zinc incorporated into the oxide layer.

Near where the zinc wire was in contact with the sample during exposure, an oxide layer containing both zinc and iron was found as shown in fig. 4.2 and table 4.1. Suggesting an iron-zinc oxide in a normal spinel structure.

4.2.1.2 Hydrazine

Hydrazine was used in two configurations with hydrogen peroxide as the oxidizing agent and without oxidizing agent relying on the oxidative properties of the solution. When hydrogen peroxide was added, the iron precipitated out of the solution and not specifically on the sample surface. When relying on the oxidative environment of the solution, working in pH 4.54, exposure ran the full 4 hours without precipitation.

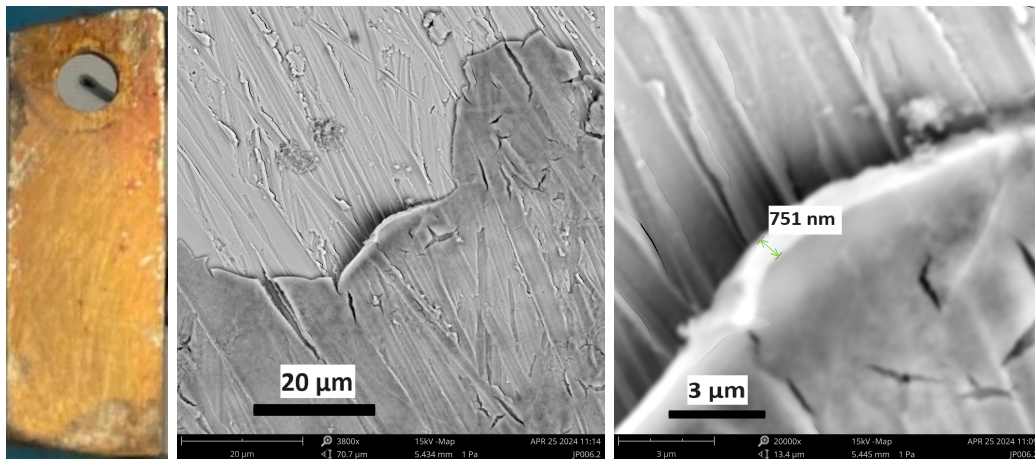


Figure 4.3: Left: Optical image of coated sample using no oxidative agent and hydrazine as pH controller. Middle: Backscatter overview of an edge of the oxide scale. Right: Measurement of thickness of the oxide scale.

As seen in fig. 4.3 the scale is approximately 750 nm thick and relatively homogeneously deposited. XRD showed slight indication of crystalline hematite (fig. 4.4)

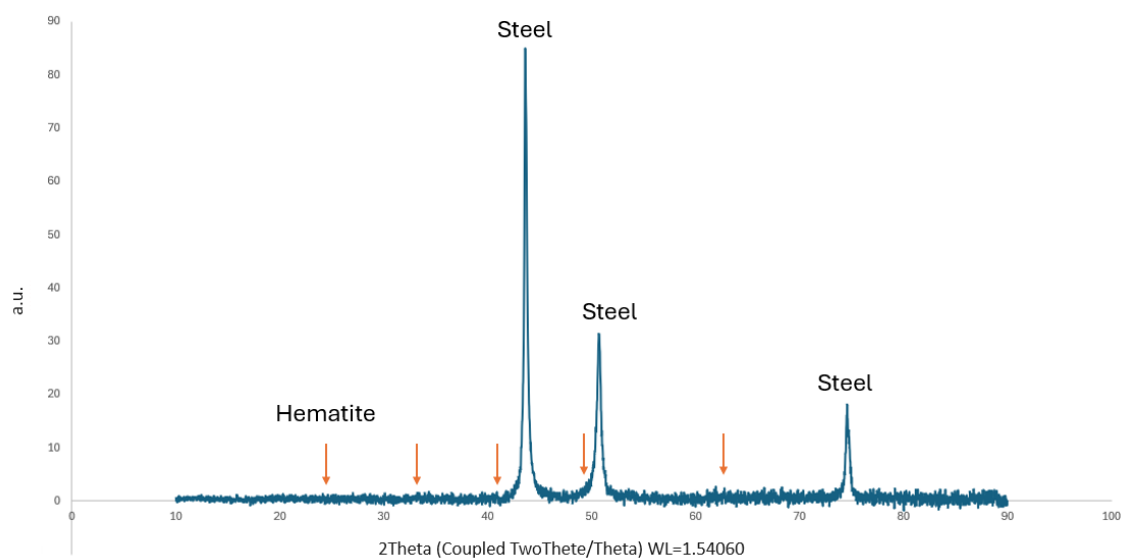


Figure 4.4: Diffractogram for sample shown in fig. 4.3, slight indication that hematite is present.

4.3 In situ iron formate

Iron formate $\text{Fe}(\text{HCOO})_2$ was produced by dissolving pure iron in formic acid, creating a colorless solution. 31.6mg of iron powder was enough to saturate the 81.35g of formic acid it was added to. Leaving it for 48h showed a white precipitation suggesting the solution was saturated and with the gas produced when dissolving the iron leaving, the process was not reversible. When replicating exposure conditions the pH was slowly raised with KOH to find a point where the iron would start to oxidize but not fully precipitate. At pH 4.5 the solution had a slight yellow tint and at pH 5.8 precipitation was rapid, pH 5 was found to be the point where rate of oxidation was most beneficial for the experiment. Target concentration of iron ions in the exposure solution was 0.358 mmol/l.

4.3.1 18-8 Stainless steel wire

4.3.1.1 KOH

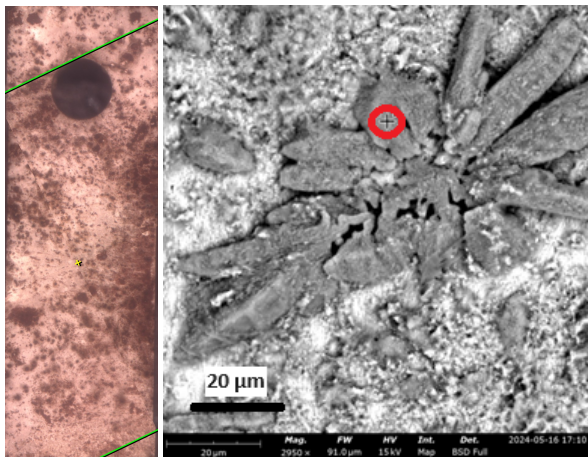


Figure 4.5: Backscatter image shows partial coverage of large crystals.

Element	Atomic Conc.	Weight Conc.
Fe	43.1	49.9
K	20.3	16.4
Cr	19.9	21.4
O	11.2	3.7
Mo	2.9	5.8
Ni	1.3	1.6
Mn	0.8	0.2

Table 4.2: EDS measurement suggests potassium is incorporated in the oxide scale.

Raising pH with KOH to the point of slight yellow tint in the solution, which occurred at pH 5, was tried in low concentration of iron ions 0.358 mmol/l and higher concentration of 3.5 mmol/l with and without oxidizing agent. Seen in fig. 4.5 and table 4.2 is without oxidizing agent and high iron ion concentration, large iron and potassium crystals were deposited. XRD analysis confirmed this (fig. 4.6).

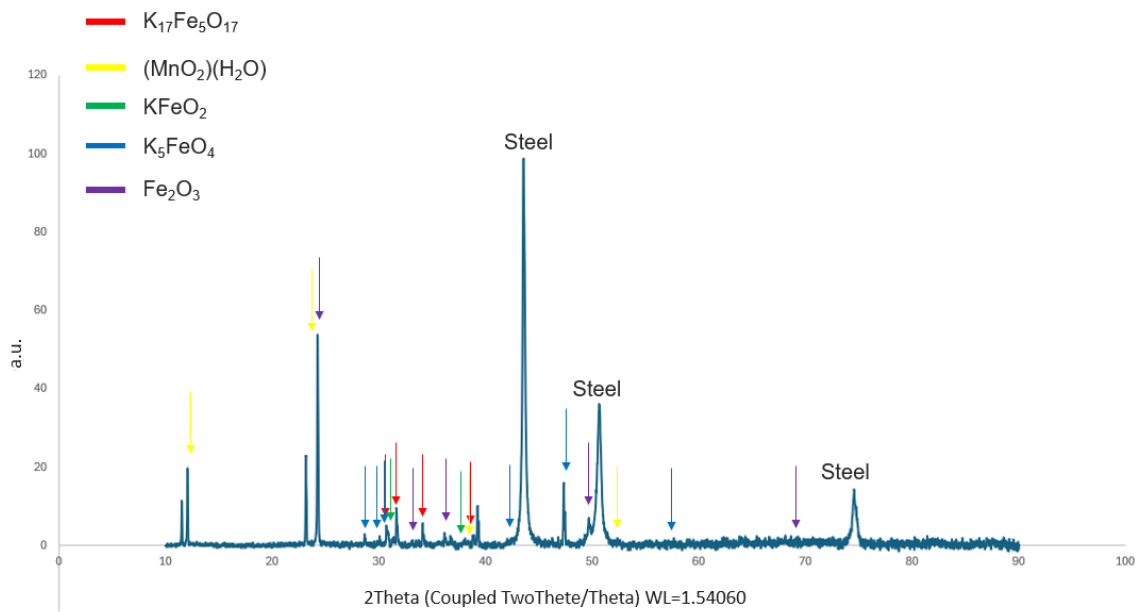


Figure 4.6: Diffractogram of sample shown in fig. 4.5 shows an array of different oxide crystals containing potassium, a few peaks were not identified.

4.3.1.2 Ammonia solution

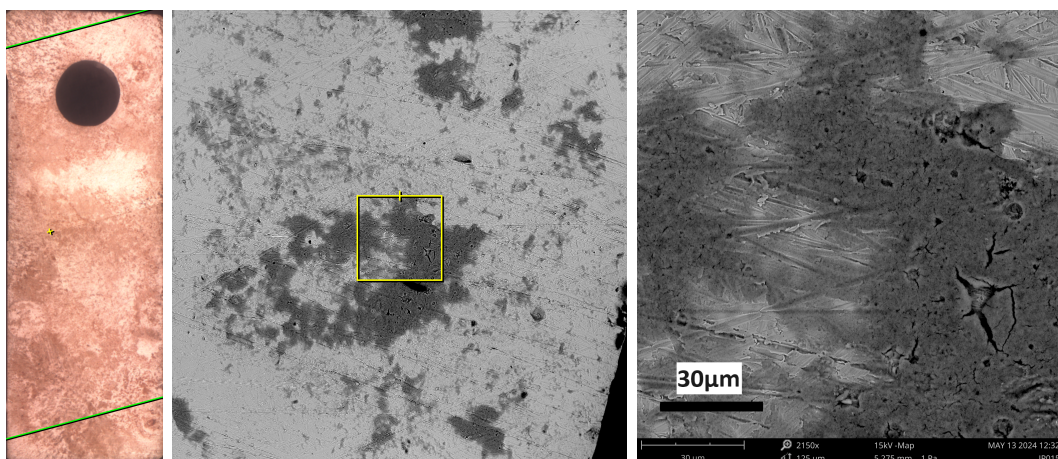


Figure 4.7: Sample laying on bottom showing partial hematite coverage. Optical left, Backscatter middle and enlarged right.

4. Results

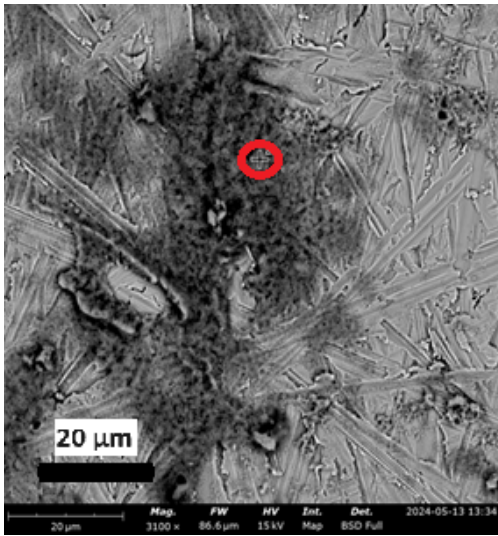


Figure 4.8: Backscatter image for spot analysis of sample in fig. 4.7.

Element	Atomic Conc.	Weight Conc.
O	52.5	24.2
Fe	37.1	59.7
Cr	4.9	7.4
Ni	2.7	4.5
Si	1.0	0.8
Mo	0.7	2.0
P	0.5	0.4
Mn	0.4	0.7
Cl	0.3	0.3

Table 4.3: EDS measurement of oxide scale.

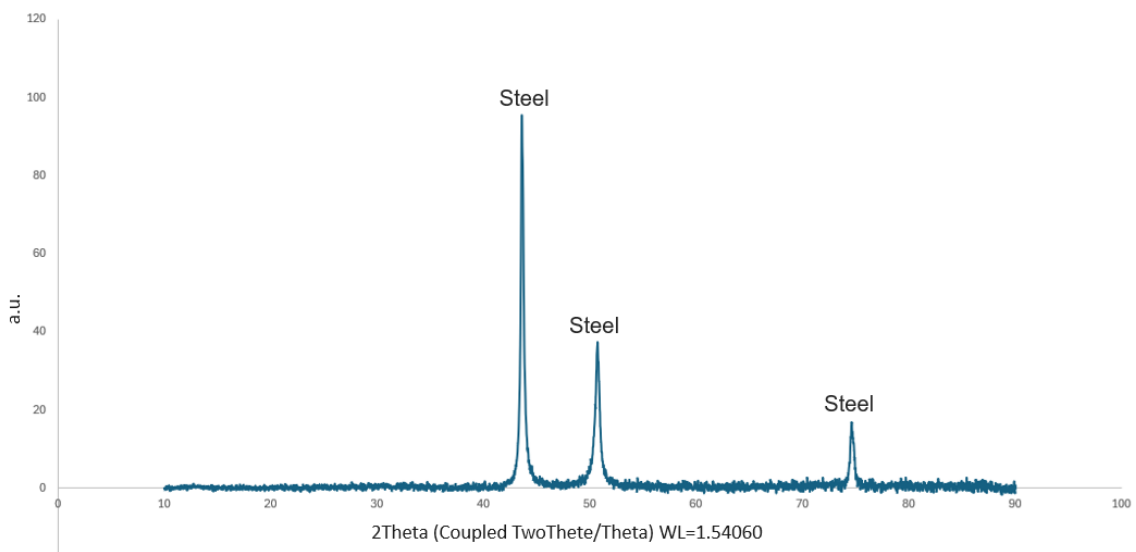


Figure 4.9: Diffractogram analysis showed no clear proof of crystalline hematite suggesting amorphous or formed oxides.

Coating produced a partial coverage as seen in fig. 4.7, the oxide scale that was produced was thick. The scale was predominantly an iron oxide as seen in fig. 4.8 and table 4.3. XRD analysis showed no crystalline hematite suggesting an amorphous oxide structure (fig. 4.9). No oxidizing agent was added to produce the coat seen in fig. 4.7

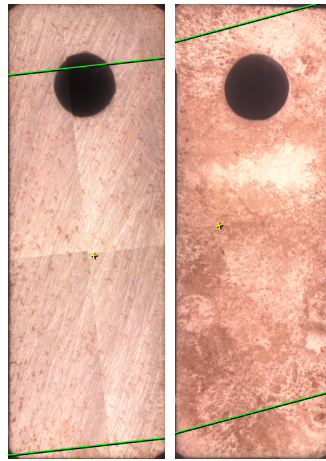


Figure 4.10: Optical image of samples from the same exposure where JP014 (left) was hung in solution in the stainless steel wire and JP015 (right) laid on the bottom of the flask.

Exposure which results shown in fig. 4.10 showing clear difference of coverage between position suggesting gravity matters when stirring moderately.

4.3.1.3 Hydrazine

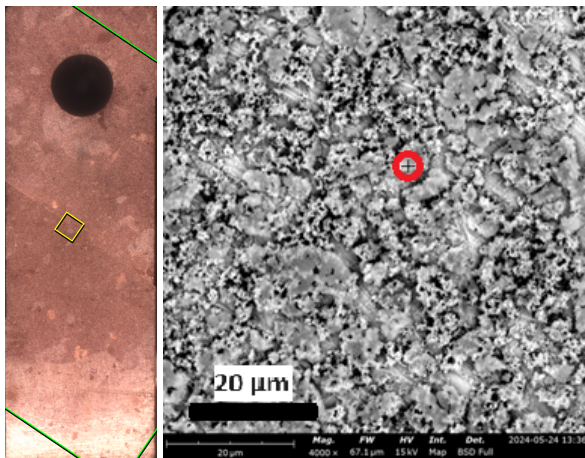


Figure 4.11: Almost full coverage of thick enough coating for the grind structure not to be visible. Optical left and backscatter for analysis right.

Element	Atomic Conc.	Weight Conc.
Fe	40.0	60.4
O	47.1	20.4
Cr	7.0	9.8
Ni	4.1	6.5
Mo	0.5	1.3
Mn	0.7	1.0
Si	0.7	0.5

Table 4.4: EDS measurement of coating.

Shown in fig. 4.11, the structure of the film was porous and coverage was satisfactory. During the exposure a layer of precipitation was formed on the surface of the solution and hematite was mainly deposited by lifting the sample out though the floating

4. Results

precipitation. EDS measurement found in table 4.4 and XRD showed clear evidence of crystalline hematite (fig. 4.12)

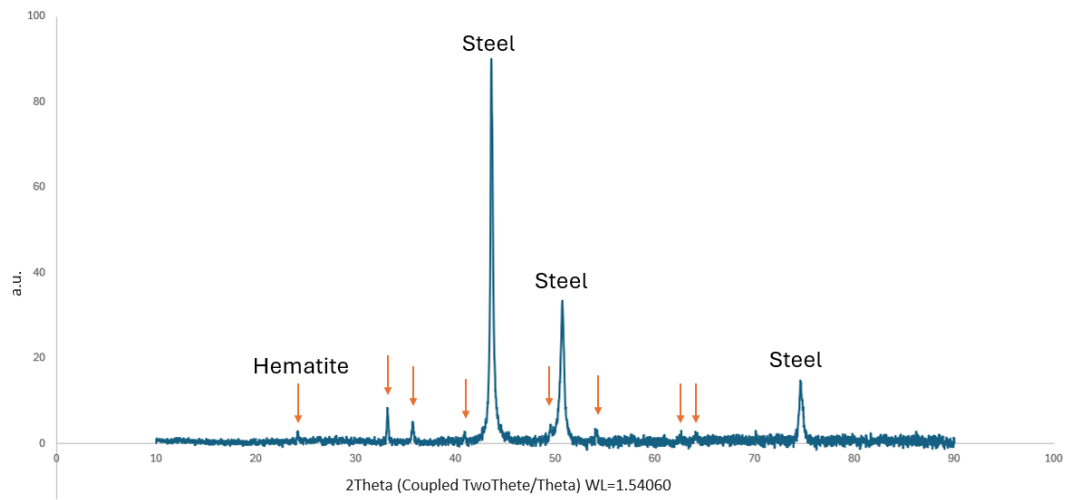


Figure 4.12: Diffractogram of the sample shown in fig. 4.11 showed clear bulk crystalline hematite.

5

Discussion

5.1 Sample position and setup

Clearly seen in fig. 4.10 is that sample position matters, this difference would likely be less with rigorous stirring making gravity's impact on result negligible. This is one among the restrictions regarding the setup used (fig. 3.1), the magnetic stirrer may not scrape the sample and this was taken great care to ensure. It was observed that after a successful exposure the flask in which the sample was exposed, had a yellow tint. Showing Fe^{III} was plentifully deposited onto the glass, this coating was very structurally sound with no heat treatment. Further testing should be conducted using a pipe sample and a steady flow to better emulate conditions of actual application. The temperature controlled oil bath made for a stable temperature in solution and continuously monitoring pH gave a clear indication to if reaction was taking place during the exposure as the pH was slowly increasing. Baking the samples in air was a decision made due to convenience, pressurized baking in normal water conditions was not at hand at the time. The impact of this should be investigated further but still it might be found that this method might be beneficial.

5.2 Hi-F Coat replication

The Hi-F method was replicated with modifications, such as excluding hydrogen peroxide, replacing iron(II)formate with iron(II)acetate and baking the sample in air instead of in pressurized water. By simplifying the process a satisfactory result was achieved even though the rudimentary setup (fig. 3.1) compared to the more advanced exposure setup (fig. 1.3) used for development of Hi-FC and OHi-FC. Furthermore in the OHi-FC, which produced the better results, surface coating was hematite heavy but showed some magnetite (fig. 1.5) while the simplified replication showed no trace of magnetite. Considering fig. 1.4 and fig. 1.5 as proof hematite is the superior cobalt uptake inhibitor, the simplified version would be suspected to perform better in a cobalt deposition test.

5.3 Ferrous ion source

5.3.1 Fe(II)Oxalate paint

Though iron oxalate was deemed unfit for the electroless deposition application due to its very low solubility in acid solution, it may form a very usable pigment in a paint. The low solubility can be explained by its polymer structure and complexing bonds shown in fig. 2.2. Creating a paint slurry to apply onto stainless steel with the required Co blocking properties would make for a cheap and easy to apply solution.

5.3.2 Iron(II)acetate

As Iron(II)acetate proved to be suitable, see section 4.2.1.2, storing proved difficult as the iron reacted with oxygen and water in air into Fe^{III}. In bulk applications this will not be a problem as no storing after opening will not be necessary.

5.3.3 Iron(II)formate

Iron(II)formate was created in house (section 2.1.3) and was the easier to work with iron source, though when dissolved in DI water it produced a notably more acidic solution than the iron(II)acetate. The lower pH starting point of iron(II)acetate results in more of the pH adjuster to be used and in larger applications this may be a financial disadvantage.

5.4 Oxidation agent

In the experiments conducted it was found redundant to use any oxidative agent due to the difficulties keeping the rate of oxidation slow enough. The opposite might though be found if running the exposure in a closed loop system, where none to little air is in contact with the solution. The need for a oxidation agent should therefore not be neglected but the possibility to exclude it is very much likely.

5.5 pH controller

Maybe the most interesting chemical to replace of the ones in the Hi-F Coat is hydrazine due to its many health and safety issues (section 1.6.2). Though it has very efficient pH and reductive properties, shown in section 4.2.1.2 and section 4.3.1.3.

5.5.1 Ammonia solution

Ammonia solution has slight reductive properties though not as potent as hydrazine. The advantage of ammonia solution is that it will not incorporate into the oxide scale. The deposited iron oxide scale proved to have a rather amorphous structure, if this is desirable or not a cobalt deposition and toughness test must decide.

5.5.2 KOH

The direct route of raising pH tried was potassium hydroxide, though it was incorporated into the oxide scale produced fig. 4.6. This is most definitely not desirable due to the complex mix of structures which makes the ability to predict cobalt deposition low.

5.6 Zinc dissolution presence

The theory of letting zinc dissolve and utilizing the evolution of H₂ gas as reducing agent was briefly touched upon. It was proved that zinc could be incorporated in the oxide scale (fig. 4.2) but further exploration on this was not pursued. The possibility of combining the zinc injection method and hematite coating should be further looked in to. Due to its double advantage of iron oxide forming normal spinel structure and Zn²⁺ being present within the cooling loop.

6

Conclusion

6.1 Hi-FC reproduction

The Hi-FC with a few modifications was reproduced with satisfactory results, the modifications were merely simplifying measures. The changes should be able to be applied in a more advanced steady flow exposure setup. The Hi-FC under simplified conditions that exclusivity produced hematite was achieved.

6.2 pH adjuster

Hydrazine, ammonia solution and potassium hydroxide were explored. Hydrazine producing the best results through sufficient coating thickness and coverage. Ammonia solution being the runner up by producing partial coverage though expected to perform better in a steady flow through a pipe exposure due to the difficulties to direct precipitation onto the sample rather than the glassware. Further experimentation the coating process using ammonia solution should be conducted. Potassium hydroxide gave unsatisfactory results by uncontrollably producing potassium ferrite oxides. Inability to control precipitates on the sample will hinder the predictability and ability to reproduce.

6.3 Iron source

Explored as iron source for use in electroless coating of hematite was iron(II)formate, iron(II)acetate and iron(II)oxalate. Freshly reacted iron(II)formate produced the best results under the conditions of this research. Dissolved iron and precipitated iron(II)formate suspended in formic acid did produce the most acidic solution to correct with the pH adjusting agent, which might be undesirable. Difficulties with storing iron(II)acetate made it produce less consistent results, something that could be avoided by careful handling and/or bulk usage. Thus, iron(II)acetate should not be disregarded as an alternative. Iron(II)oxalate was not fit for use in electroless deposition, but as mentioned has the potential to be used as pigment in a paint slurry. The feasibility to create such a paint was not further explored.

Bibliography

- [1] Yan Ma, Chang Qin, Jiawei Chen, Xinxin Li, Zhixin Zhang, and Liying Zhang. Influence of zinc injection on deposition of corrosion products on inner wall of heat transfer tube. *International Journal of Advanced Nuclear Reactor Design and Technology*, 3(June):139–144, 2021. ISSN 24686050. doi: 10.1016/j.jandt.2021.07.003. URL <https://doi.org/10.1016/j.jandt.2021.07.003>.
- [2] Hideyuki Hosokawa, Makoto Nagase, and Motomasa Fuse. Development of a Suppression Method for Deposition of Radioactive Cobalt after Chemical Decontamination : (I) Effect of the Ferrite Film Coating on Suppression of Cobalt Deposition Development of a Suppression Method for Deposition of Radioactive Cobalt. *Journal of Nuclear Science and Technology*, 3131(I), 2012. doi: 10.1080/18811248.2010.9711975.
- [3] Jiaxin Chen. Plant piping radioactivity suppression through prefilming. Technical report, 2021.
- [4] Valentina Cantatore, Christine Geers, Jiaxin Chen, and Itai Panas. Insights into the zinc effect on radio-cobalt deposition on stainless steel piping surfaces under BWR conditions from experiment guided 1st principles modelling. *Journal of Nuclear Materials*, 540(November), 2020. doi: 2020.152361.
- [5] Nasser Kanani. *Electroplating - Basic Principles, Processes and Practice*. Autotech Deutschland GmbH, 2004.
- [6] F Roumiguère. Field Experience on Zn Injection on PWR Plants With a View to Dose Rate Reduction. pages 1–9, 2005.
- [7] Thimgren; Hanna Ölander Gür Stig, Erixon; Thommy, Godås; Peter, Hofvander; Ingemar, Lund; Lars, Malmqvist; Ingela. Strålskydd vid svenska kärnkraftverk under perioden 1994-2002, samt reflexioner om kommande utveckling. *SSI Rapport*, 2003.
- [8] Tsuyoshi Ito, Hideyuki Hosokawa, Makoto Nagase, and Motomasa Fuse. Development of a suppression method for deposition of radioactive cobalt after chemical decontamination : (III) the suppression mechanism with preoxidized ferrite film for deposition of radioactive cobalt. *Journal of Nuclear Science and Technology*, 3131(Iii), 2013. doi: 10.1080/00223131.2013.814900.
- [9] SIGMA-ALDRICH. Material Safety Data Sheet Hydrazine, 2014.
- [10] Cristina M. Oropeza. An Evaluation Study Of The Effectiveness Of Using A

- Reaction An Evaluation Study Of The Effectiveness Of Using A Reaction based Process For Hydrazine Waste Remediation, 2011.
- [11] Western Oregon University. No Title. URL <https://people.wou.edu/~cournna/ch412/pourbaix.htm>.
- [12] National Center for Biotechnology Information. PubChem Compound Summary for CID 9321, Hydrazine. 3:1–138, 2024. URL <https://pubchem.ncbi.nlm.nih.gov/compound/Hydrazine>.
- [13] Compound Summary for CID 222, Ammonia, 2024. URL <https://pubchem.ncbi.nlm.nih.gov/compound/Ammonia>.
- [14] Shuo Yin, Richard Wirth, Hongping He, Changqian Ma, Jiayong Pan, Jieqi Xing, Jiannan Xu, Jiali Fu, and Xia Nan Zhang. Replacement of magnetite by hematite in hydrothermal systems: A refined redox-independent model. *Earth and Planetary Science Letters*, 577:117282, 2022. ISSN 0012821X. doi: 10.1016/j.epsl.2021.117282. URL <https://doi.org/10.1016/j.epsl.2021.117282>.
- [15] Curtis W. Kovach. High-Performance Stainless Steels.
- [16] A. Bogner, P. H. Jouneau, G. Thollet, D. Basset, and C. Gauthier. A history of scanning electron microscopy developments: Towards "wet-STEM" imaging. *Micron*, 38(4):390–401, 2007. ISSN 09684328. doi: 10.1016/j.micron.2006.06.008.
- [17] Shijing Zhang, Junwei Xu, Chengxin Lu, Rumeng Ouyang, Jiamei Ma, Xusheng Zhong, Xiuzhong Fang, Xianglan Xu, and Xiang Wang. Preparation method investigation and structure identification by XRD and Raman techniques for A2B2O7 composite oxides. *Journal of the American Ceramic Society*, 107(5): 3475–3496, 2023. ISSN 15512916. doi: 10.1111/jace.19645.
- [18] B. E. Warren. *X-ray Diffraction*. Dover Publications, 1990.

DEPARTMENT OF SOME SUBJECT OR TECHNOLOGY
CHALMERS UNIVERSITY OF TECHNOLOGY
Gothenburg, Sweden
www.chalmers.se



CHALMERS
UNIVERSITY OF TECHNOLOGY